Ergonomics

ISSN: 0014-0139 (Print) 1366-5847 (Online) Journal homepage: http://www.tandfonline.com/loi/terg20

Measuring exertion time, duty cycle and hand activity level for industrial tasks using computer vision

Oguz Akkas, Cheng Hsien Lee, Yu Hen Hu, Carisa Harris Adamson, David Rempel & Robert G. Radwin

To cite this article: Oguz Akkas, Cheng Hsien Lee, Yu Hen Hu, Carisa Harris Adamson, David Rempel & Robert G. Radwin (2017) Measuring exertion time, duty cycle and hand activity level for industrial tasks using computer vision, Ergonomics, 60:12, 1730-1738, DOI: 10.1080/00140139.2017.1346208

To link to this article: http://dx.doi.org/10.1080/00140139.2017.1346208

Accepted author version posted online: 22 Jun 2017.
Published online: 06 Jul 2017.

ERGONOMICS, 2017
VOL. 60, NO. 12, 1730–1738
https://doi.org/10.1080/00140139.2017.1346208

Taylor & Francis
Taylor & Francis Group

Measuring exertion time, duty cycle and hand activity level for industrial tasks using computer vision

Oguz Akkas[a], Cheng Hsien Lee[b], Yu Hen Hu[b], Carisa Harris Adamson[c], David Rempel[c] and Robert G. Radwin[a]

[a]Department of Industrial and Systems Engineering, University of Wisconsin-Madison, Madison, WI, USA; [b]Department of Electrical and Computer Engineering, University of Wisconsin-Madison, Madison, WI, USA; [c]Department of Medicine, University of California, San Francisco, San Francisco, CA, USA

ABSTRACT

Two computer vision algorithms were developed to automatically estimate exertion time, duty cycle (DC) and hand activity level (HAL) from videos of workers performing 50 industrial tasks. The average DC difference between manual frame-by-frame analysis and the computer vision DC was −5.8% for the Decision Tree (DT) algorithm, and 1.4% for the Feature Vector Training (FVT) algorithm. The average HAL difference was 0.5 for the DT algorithm and 0.3 for the FVT algorithm. A sensitivity analysis, conducted to examine the influence that deviations in DC have on HAL, found it remained unaffected when DC error was less than 5%. Thus, a DC error less than 10% will impact HAL less than 0.5 HAL, which is negligible. Automatic computer vision HAL estimates were therefore comparable to manual frame-by-frame estimates.

Practitioner Summary: Computer vision was used to automatically estimate exertion time, duty cycle and hand activity level from videos of workers performing industrial tasks.

ARTICLE HISTORY
Received 14 February 2017
Accepted 19 June 2017

KEYWORDS
Computer vision; automated exposure analysis; repetitive motion; work related musculoskeletal disorders; exposure assessment

1. Introduction

Quantification of exposure variables such as repetition, duration and duty cycle (DC) are important for evaluating risk and for the prevention of work-related musculoskeletal disorders (Latko et al. 1997; Spielholz et al. 2001; Punnett and Wegman 2004; Bao et al. 2006; Marras et al. 2009; Silverstein et al. 2010; Burt et al. 2011; Harris-Adamson et al. 2015). Assessment methods available for quantifying job physical risk factors include self-reports, observation, video-based single frame analysis and direct measurement. Among these methods, observation is among the most widely used in both research and industry practice (Ebersole and Armstrong 2002; David 2005; Dempsey et al. 2005, Spielholz et al. 2008; Paulsen et al. 2014).

The American Conference for Government Industrial Hygienists (ACGIH) threshold limit value (TLV) for hand activity is one commonly used observational method (ACGIH Worldwide 2001) and is based on hand activity level (HAL) and force. HAL is quantified using a visual-analogue scale anchored between 0 (hand idle most of the time) and 10 (rapid, steady motions/exertions; difficulty keeping up) (Latko et al. 1997). The TLV for hand activity also has a table whereby objective measures of frequency and duty cycle can be used to calculate HAL, or an equation may be used for calculating HAL using the same variables (Radwin et al. 2015).

Video frame-by-frame coding is the accepted gold standard for quantifying frequency and duty cycle, and is considered more accurate and reliable compared to observer estimation (Fan et al. 2014). Computer software, such as Multimedia Video Task Analysis® (MVTA), is a widely-used method (Yen and Radwin 1995; Lu, Sudhakaran, and Aep 2005; Yen and Radwin 2006; Bao et al. 2006; Paquet, Mathiassen, and Dempsey 2006; Lu et al. 2008; Dartt et al. 2009; Chang et al. 2010; Story et al. 2010; Burt et al. 2013; Coelho et al. 2013; Harris-Adamson et al. 2013; McGaha et al. 2014; Estember, Panugot, and Vale 2015; Dale et al. 2016). Once annotated, DC is calculated as the percent exertion time divided by the total time. Similarly, the frequency is calculated by counting the total number of hand exertions in a cycle, divided by the cycle time (Latko et al. 1997; Radwin et al. 2015). An exertion involves an action where the hand produces a force greater than five per cent of maximum for a particular posture, as defined in the TLV (ACGIH Worldwide 2001). Akkas et al. (2015) developed an equation based on the average RMS speed of the moving hand during exertions, and DC to automatically calculate HAL.

CONTACT Robert G. Radwin radwin@discovery.wisc.edu

Although video frame-by-frame coding is accurate and precise, it is often tedious and time consuming, and thus less preferred by practitioners (David, 2005). The primary aim of the current research is to automate the process of measuring hand activity using computer vision. Our laboratory previously developed an efficient cross-correlation template matching algorithm to track a worker's hand while performing a repetitive task (Chen et al. 2013). An algorithm to automatically calculate the DC utilized threshold crossings of velocity and acceleration signals. The determination of exertion and rest states was made by looking at acceleration between two local velocity minima points. A threshold was determined through trial and error, and an exertion started when the acceleration was greater than the threshold and was sustained until the acceleration was less than the threshold. This attempt to automate the DC calculation however was limited to the specific load transfer task performed. When applying the same algorithm to a different task, the algorithm failed (Akkas et al. 2016).

Another set of algorithms considered more global features to determine when a participant was exerting force for a simple repetitive load transfer task in the laboratory (Akkas et al. 2016). The decision tree (DT) algorithm determined if there was any change in the trajectory, speed and acceleration. If a change was detected, location information and the velocity threshold was used to determine if the change represented a transition from an exertion state to rest, or vice versa. The feature vector training (FVT) algorithm was adapted from the k-nearest neighbourhood classifier, where the first cycle of each task was used as the training template for the remaining cycles of the task. We also trained the FVT algorithm using several cycles of a given task. The average difference between manual frame-by-frame analysis and computer vision using the DT algorithm was 2.7%. The FVT algorithm had a 3.3% average difference when trained using the first cycle sample of each repetitive task, and had a 2.8% average difference when trained using several representative repetitive cycles (Akkas et al. 2016).

The current study applies these methods to videos of workers performing actual industrial tasks. Industrial tasks were selected from Harris et al. (2011), and the DT and FVT algorithms were used for calculating exertion time, DC and HAL. We hypothesise that the algorithms we developed for automatic computer vision measures of DC for industrial tasks are comparable to manual frame-by-frame estimates. This hypothesis is tested by analysing 50 industrial tasks using manual and automatic methods, and comparing the resulting measures.

2. Methods

2.1. Video clip selection

The selected videos were limited to having at least five contiguous cycles, no breaks in the video, little camera motion and no visual obstructions. Videos with a partially obstructed view were deemed suitable for the automated analysis when the hand was blocked, but there was enough of the arm visible to determine the location of the hand. Videos with small breaks were deemed suitable if the break was outside of the primary task. Based these criteria, 50 tasks were selected. Exertion time and cycle time were calculated using MVTA single-frame video analysis (i.e. ground truth) and frequency, and DC were calculated based on these measures. Exertions included all pinches or power grips, rather than the 'heavy' pinch or power grip levels reported in Harris et al. (2011). Observed HAL values were the same used in Harris et al. (2011), which were evaluated based on human observation of the task. A summary of these task characteristics are provided in Table 1.

2.2. Hand tracking and camera motion compensation

After the video clips were selected based on the above criteria, the hand tracking algorithm (Chen, Hu, and Radwin 2014) was used to track the most active hand. Analysts determined the most active hand based on the greatest HAL scores and visibility of the hand. Once determined, the most active hand was tracked and the hand location was scaled using hand breadth data as described in Akkas et al. 2015, 2016. The RMS speed summary data are given in Table 1.

Unlike the stationary camera used in the laboratory, the industrial videos were recorded using hand-held cameras. Therefore, the videos shook and sometimes the viewing angles changed over time. These factors made the tracking of the hand trajectory irregular, and increased the difficulty of estimating the DC by tracking hand trajectory alone. To compensate for the motion of the camera, we identified a geometric transformation between every couple of successive frames. Given two successive frames, we detected the speed up robust features (Bay, Tuytelaars, and Van Gool 2006) and extracted the matched points using sum of squared differences as our feature matching metric. We applied the Matlab function, estimate *GeometricTransfrom*, to calculate the affine transform matrix between the matched points. This function excludes outliers using the M-estimator sample consensus algorithm (Torr and Zisserman 2000), which is a variant of the random sample consensus algorithm (RANSAC) (Fischler and Bolles 1981).

Table 1. Ground truth summary statistics for 50 industrial tasks.

	Frequency (Hz)	RMS speed (mm/s)	Duty cycle (%)	Observed HAL (0–10)
Min	0.135	260.6	46.3	2
Max	1.16	1347.6	95.6	8
Median	0.6	675.8	72.9	5

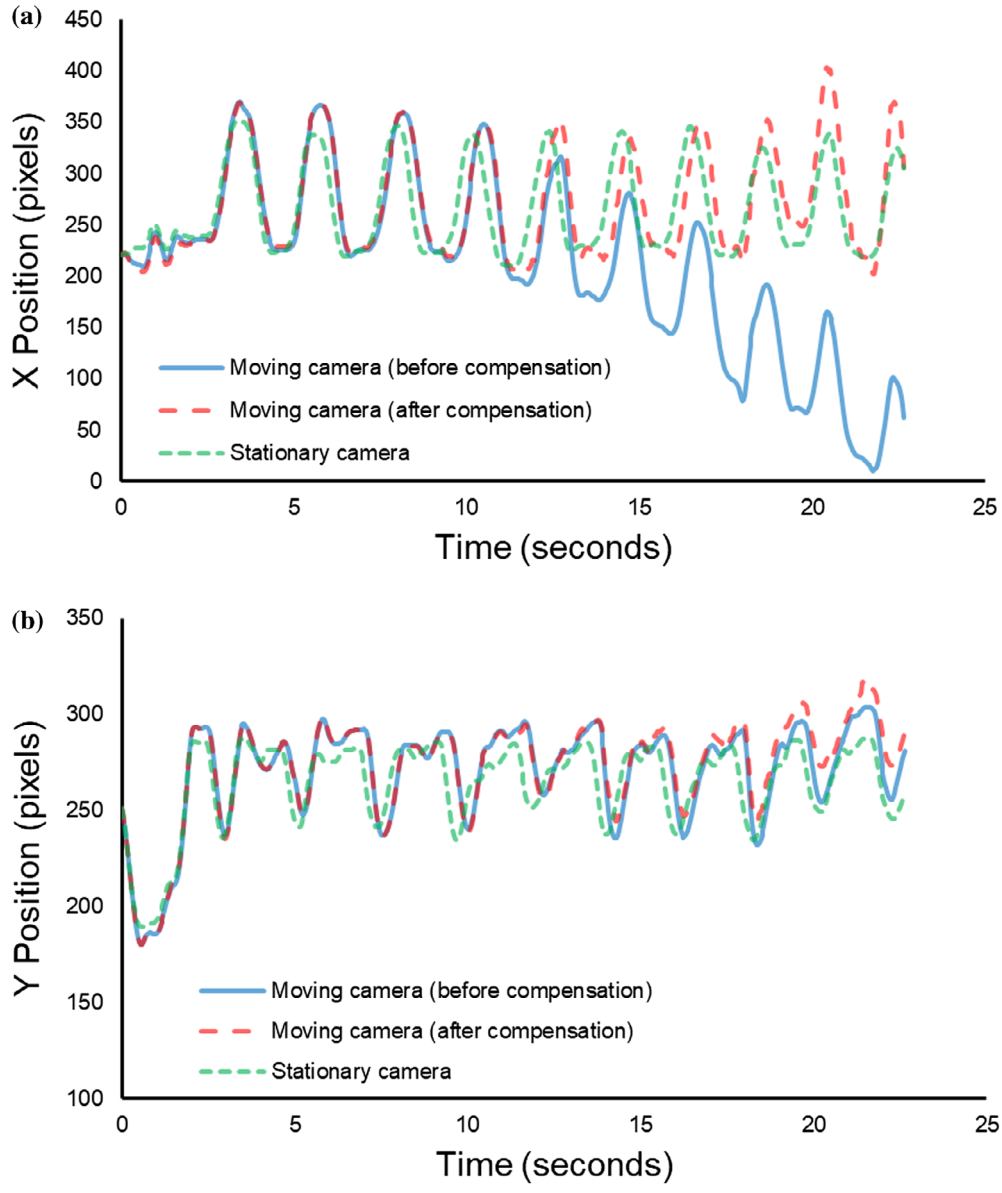

Figure 1. The hand trajectories of a stationary camera and moving camera before and after camera motion compensation in the (a) *x*-direction and (b) *y*-direction.

Assuming the transform matrix between the *i*-th frame and the $(i+1)$-th frame is T_i, the cumulative transformation of the $(i+1)$-th frame and the first frame will be the product of T_1 to T_i, which is

$$H_{i+1} = \prod_{n=i}^{1} T_i$$

Then, we can compute the compensated hand coordinate of the *i*-th frame, (x_{ic}, y_{ic}), by

$$\begin{bmatrix} x_{ic} & y_{ic} & 1 \end{bmatrix} = \begin{bmatrix} x_i & y_i & 1 \end{bmatrix} \times H_i$$

where (x_i, y_i) is the tracking hand coordinate before compensated. Notice that the transform operators are 3×3 matrices. The closer the matched points were located to the plane of motion of the tracked hand, the better the performance of the camera motion compensation.

To demonstrate the effects of the camera motion compensation algorithm, two cameras recorded the same task at the same time in the laboratory. One camera was stationary and the other moved horizontally at an approximately constant speed. The task involved a subject transferring tennis balls from one bin to another, perpendicular to the video plane of the cameras.

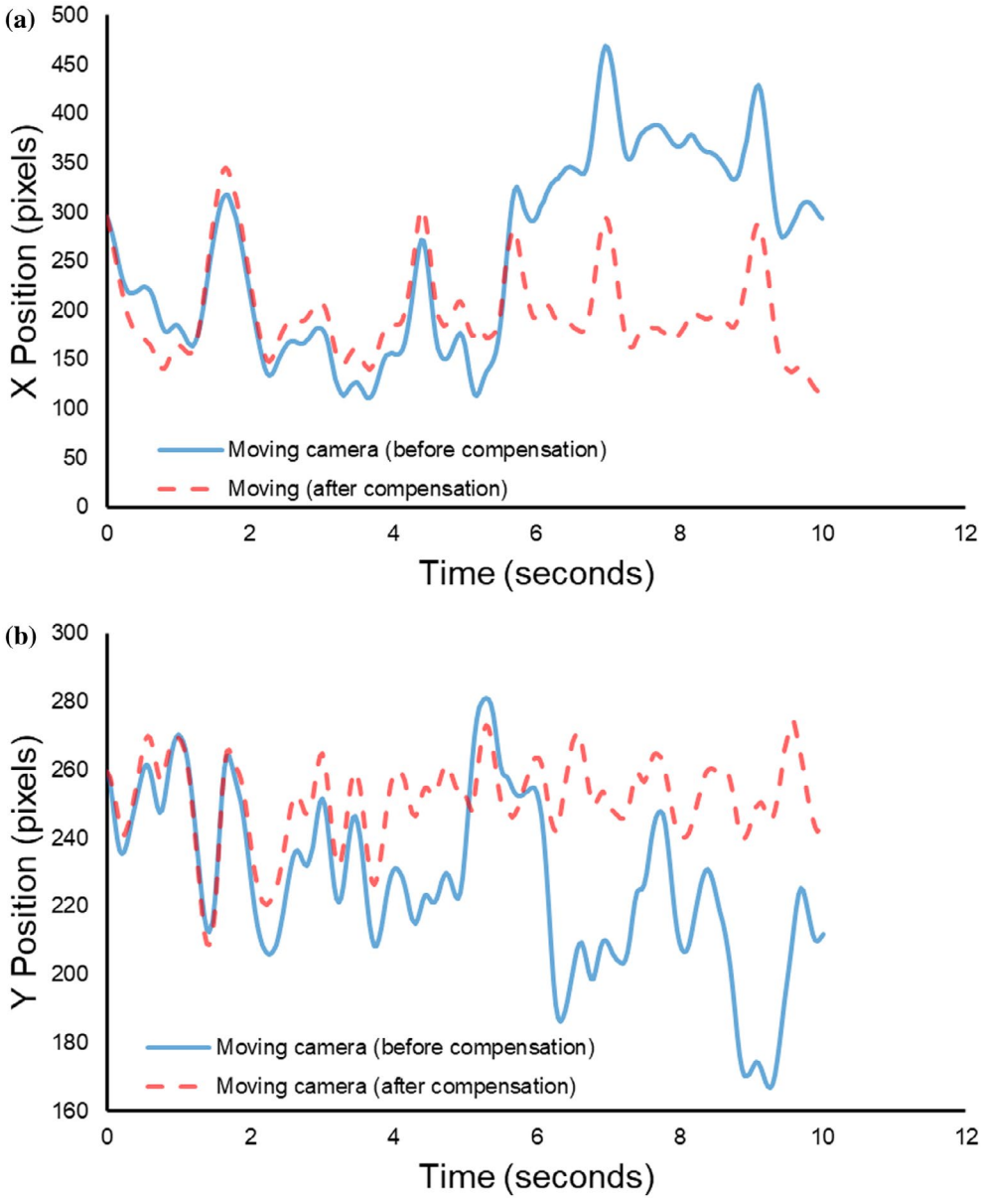

Figure 2. The hand trajectories before and after camera motion compensation in the (a) horizontal (*x*)direction and (b) vertical (*y*) direction.

The horizontal (*x*) and vertical (*y*) directions of the hand trajectories for the moving camera before and after camera motion compensation, and the hand trajectories for the stationary camera as ground truth, are shown in Figure 1. Observe that the hand trajectories for the moving camera after compensation were closer to the hand trajectories of the stationary camera.

An example of the *x* and *y* direction hand trajectories before and after camera motion compensation from an industry video are shown in Figure 2. Since there was no stationary camera used in the industry videos, there was no ground truth signal to compare against. However, observe that the hand trajectories tend to concentrate in a smaller range after the camera motion compensation, which is closer to a situation where the camera is stationary.

Table 2. Duty cycle estimate error summary (%).

	Decision tree algorithm		Feature vector training algorithm	
	All videos	All videos after compensation	All videos	All videos after compensation
Max	43.05	22.11	30.62	36.54
Min	0.08	−43.05	−40.88	−43.25
Mean	14.22	−5.76	3.33	1.44
SD	10.35	13.37	15.10	16.09

Table 3. HAL estimate error summary (HAL units).

	Decision tree algorithm		Feature vector training algorithm	
	All videos	All videos after compensation	All videos	All videos after compensation
Max	2.58	2.50	2.88	3.18
Min	−0.51	−1.42	−1.45	−1.37
Mean	0.86	0.48	0.38	0.30
SD	0.75	0.86	0.92	0.90

2.4. Decision tree algorithm

The DT algorithm used kinematic properties measured from the hand tracking signal (i.e. location, speed and acceleration) to determine when an exertion was made. The DT algorithm does not require any training. Peak curvature scores (Rao, Yilmaz, and Shah 2002; Akkas et al. 2016), which represent significant changes in the trajectory and kinematic signals were calculated. These changes occurr during transitions between different states (i.e. Grasp-Move, Move-Release). However, the signals were sometimes noisy due to the variable nature of human motion. Consequently, not all peak curvature scores represented state changes. We therefore utilized velocity and location signals as described in Akkas et al. 2016. Detailed steps of the training-based DC estimation algorithm are summarised in Algorithm 1:

Algorithm 1. Decision Tree Algorithm

inputs: feature vectors, video frame number from hand tracking

output: states (Get or Put) for each video frame

(1) Find local maxima curvature index values and associated frames.
(2) For each frame, check if the frame has local maxima curvature index point.
(3) If a frame is identified as a local maxima, then check the location that corresponds to the frame number to see if the location is inside a grasp region or release region. If the location is inside one of these regions then use the previous state to annotate as next state (Put if previous state was Get, or Get if previous state was Put).
(4) If above criteria does not apply, check the corresponding velocity and compare to the velocity threshold. If the current velocity is under threshold, then use the previous state (Put if previous state was Get, or Get if previous state was Put).
(5) If none of above criteria applies, then annotate as same state as the previous one.

2.5. FVT Algorithm

The FVT algorithm was trained using corresponding phases (i.e. exertion and rest) based on the first cycle of each video clip. The first cycle phases of videos that were manually annotated using MVTA were inputted for the first cycle exertion and rest elemental times.

There was a wide range of cycle times among the tasks, ranging from less than one second to more than ten seconds. A short first cycle might only be ten frames. Since only one cycle was used for training, feature selections by cross validation methods were infeasible. Instead of selecting a best subset of features, we used of the all hand trajectory features which included location, velocity, speed, acceleration, acceleration magnitude and spatiotemporal curvature.

We applied the k-nearest neighbour (kNN) classifier as the state estimator. In a kNN classifier, all training data (feature vectors) and corresponding classifications (exertion and rest) are used for the classifier. For each test feature vector, a set of k (usually chosen as an odd number) training vectors that are most similar to the test vector are identified using a similarity metric. Then the training vector dominant label (by majority voting of the k labels) is assigned to the test vector. We used $k = 1$ since we only had one cycle of samples for the training data. Detailed steps of the training based DC estimation algorithm are summarised in Algorithm 2:

Algorithm 2. Feature Vector Tarianing Algorithm

Training Phase

inputs: feature vectors, state labels (Get and Put)

(1) Nomalise all features into zero mean and unit variance, and store the normalisation factors for testing phase.
(2) Train the k-nearest neighbourhood classifier by using the chosen feature vectors and the MVTA labels of the training data.

Test Phase

inputs: frame number, feature vectors

output: states (Get or Put) for each frame

(1) Normalise all features with the normalisation factors from training phase.
(2) Input the feature vectors into the classifier trained in the training phase frame by frame to classify each frame to be Get or Put.
(3) The estimated duty cycle is computed by (# of Put)/((# of Get) + (# of Put))

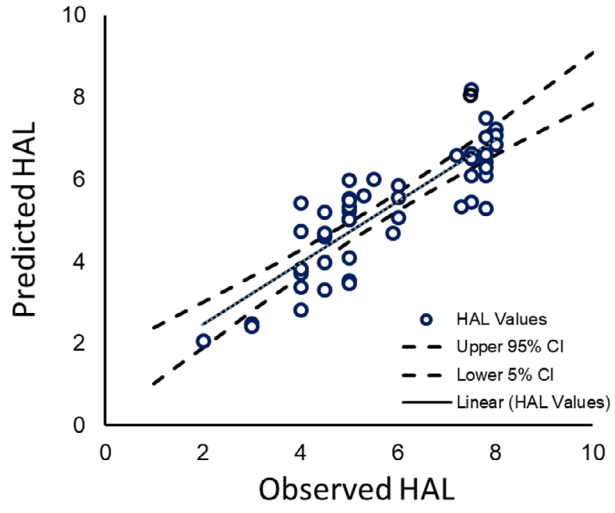

Figure 3. Estimated HAL versus observer HAL (Decision Tree algorithm).

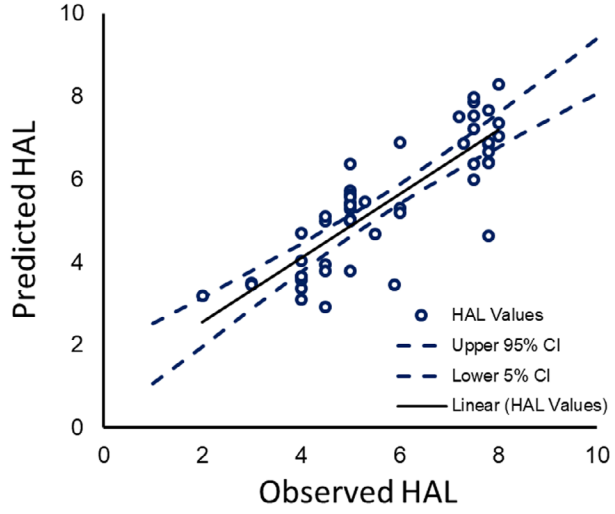

Figure 4. Estimated HAL versus observer HAL (The First Cycle Training algorithm).

3. Results

3.1. DC and corresponding HAL estimates

The DC estimate error (%) was calculated as the average difference between the manual frame-by-frame ground truth DC (%) and the computer vision estimated DC (%). Summary statistics of the DC estimate error is provided in Table 2 for the DT and FVT algorithms. We also calculated the HAL estimate error as the average difference between the observer HAL and predicted HAL in Table 3. The HAL was computed using the HAL equation, given the corresponding RMS speed and DC. The results before and after camera motion compensation are all listed for comparison.

We show a scatter plot of predicted HAL vs. observer HAL after camera motion compensation in Figure 3 for the DT algorithm, and in Figure 4 for the first cycle FVT algorithm. The regression equation for the DT algorithm was:

$$\text{Predicted HAL} = 0.75\ \text{Observer HAL} + 0.94,\ R^2 = 0.72$$

and the regression equation for the FVT algorithm was:

$$\text{Predicted HAL} = 0.77\ \text{Observer HAL} + 1.00,\ R^2 = 0.70$$

A histogram of the HAL estimate error after camera motion compensation is shown in Figure 5 for the DT algorithm and Figure 6 for the first cycle FVT algorithm.

4. Discussion

In this study, we applied the DT and FVT algorithms from Akkas et al. (2016) to a variety of industrial tasks. We tested 50 tasks and the average DC error was −5.76% for the DT algorithm and 3.3% for the FVT algorithm. The average HAL error was 0.48 for the DT algorithm and 0.30 for the FVT algorithm.

One of the assumptions for the FVT algorithm was that the tasks involved mono-cycle repetitive hand motions. Some tasks that do not have stereotypical cycles such as

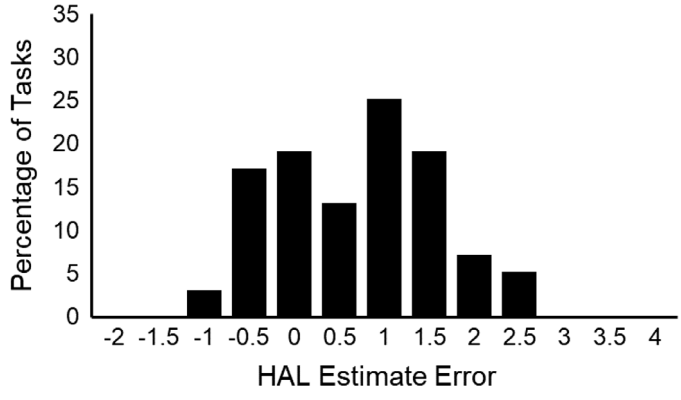

Figure 5. Histogram of the HAL estimate error (Decision Tree algorithm).

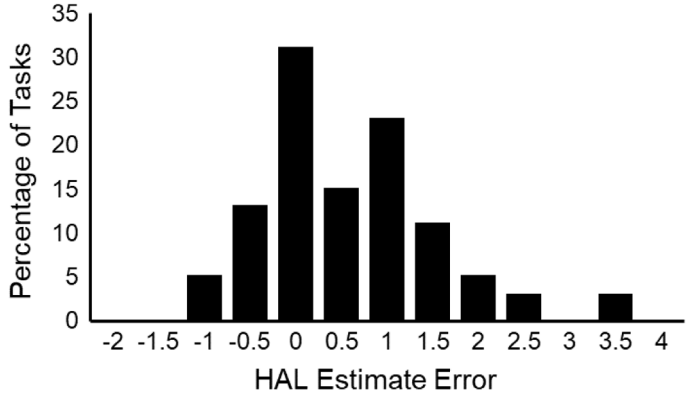

Figure 6. Histogram of the HAL estimate error (The First Cycle Training algorithm).

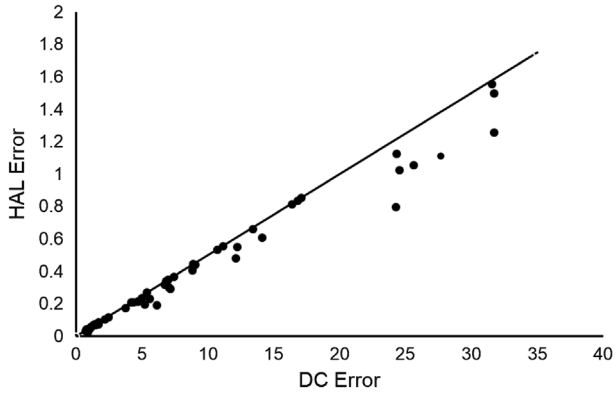

Figure 7. HAL estimate error versus DC estimate error. Each point represents a video. It verifies that $|\Delta(\text{HAL})| \leq 0.05 \cdot |\Delta(\text{DC})|$ since all points are below the $y = 0.05x$ line.

sewing are usually challenging. The larger DC estimate errors might come from the larger deviation of motions for different cycles in the videos. Selecting a representative cycle for the task or more than one cycle for training the algorithm might help alleviate these errors.

Consider the speed and duty cycle based the HAL speed equation from Akkas et al. (2015):

$$\text{HAL} = 10 \cdot \left[\frac{e^{-15.87+0.02\,\text{DC}+2.25 \ln S}}{1 + e^{-15.87+0.02\,\text{DC}+2.25 \ln S}} \right]$$

where s is RMS speed in mm/s.

If $y = 15.87 + 0.02 \cdot DC + 2.25 \ln S$, then $\text{HAL} = 10 \cdot e^y / (1 + e^y)$, or

$e^y = (\text{HAL})/(10 - \text{HAL})$, and $1/(1 + e^y) = (10\text{-HAL})/10$.

Furthermore, $de^y/d(DC) = e^y \cdot (0.02)$.

Hence:

$$\frac{d(\text{HAL})}{d(\text{DC})} = \frac{d(\text{HAL})}{de^y} \cdot \frac{de^y}{d(\text{DC})} = \frac{10}{(1+e^y)^2} \cdot e^y \cdot (0.02)$$

$$= 10 \cdot \left(\frac{10-\text{HAL}}{10} \right)^2 \cdot \frac{\text{HAL}}{10-\text{HAL}} \cdot (0.02) = 0.002 \cdot (\text{HAL}) \cdot (10-\text{HAL})$$

Since $0 \leq \text{HAL} \leq 10$, then $(\text{HAL}) \cdot (10\text{-HAL}) \leq 25$, where the maximum occurs when HAL = 5. Therefore, a change of DC will affect the HAL value, bounded by:

$$|\Delta(\text{HAL})| \leq 0.05 \cdot |\Delta(\text{DC})|$$

When $|\Delta(\text{HAL})| \geq 0.5$, the rounded HAL value to the nearest integer will be erroneous, thus, as long as $|\Delta\text{DC}| < 10\%$, the estimate HAL value will be correct, assuming the speed estimate s is correct. Note that DC in this equation is actually a relative error (ranging from 0 to 100%). Therefore, the HAL estimation error is sensitive to the relative estimation error of DC.

Based on the sensitivity analysis, we showed that the HAL estimate error should be less than 0.05 times the DC estimate error. That means a DC estimate error less than 10% could achieve a HAL error less than 0.5. The HAL estimate error vs. the DC estimate error for all of the videos is plotted in Figure 7. For this figure, the HAL estimate error is calculated from speed formula, keeping speed fixed and using ground truth duty cycle and estimated duty cycle. All of the data points are all located below the line of $y = 0.05x$, which verifies that conclusion. Having less than 10% DC error gives less than 0.5 HAL error, assuming no errors in the speed estimation. Consequently, the DC error for HAL estimation is almost negligible.

We used the DC error, which was the difference between the ground truth DC and the estimated DC, as the criterion to estimate performance. That might not accurately represent the algorithm performance, since false alarms and missed detections would cancel each other out. That means the algorithm having the minimum DC estimate error might not have the best classification rate.

The ground truth states are usually consecutive GET states followed by consecutive PUT states. The FVT algorithm estimated whether the current state was GET or PUT on a frame by frame basis, which didn't utilize temporal information. Conversely, the DT algorithm examined the local maxima of spatiotemporal curvature to determine

the transitions between GET and PUT states. The accuracy of the DC estimation might improve if we combined the advantages of both algorithms.

The camera motion compensation improved mean DC by 8.46% for the DT algorithm and by 1.98% for the FVT algorithm. Since the DT algorithm used curvature scores for state changes, compensation might affect the false state changes. For the industry videos, the camera motion compensation algorithm selected matched points automatically; however, manual selection of matched points may yield better compensation.

Our findings indicate that HAL can be estimated accurately and reliably using DC and speed. Confidence intervals were added to the regression line to indicate the margin of error for the HAL estimation. Although there were differences between the estimated HAL values in comparison to the subjective judgement of human observers, the range of these differences is considered small. The First Cycle Training algorithm had the least HAL error (Figure 6). The algorithm tended to overestimate smaller HAL values and underestimate larger HAL values however these differences are small. For example, when observed HAL = 2, the predicted HAL was 0.4 units greater, and when observed HAL = 8, the predicted HAL was less than 1 unit less. On average the HAL errors were less than one HAL unit (Table 3). Although on occasion the errors exceed one HAL unit, the frequency of these errors was small, as shown in Figures 5 and 6.

Although the observer HAL was used as ground truth, it is not known if these differences are due to limits of human judgement or due to the computer vision algorithms. The ability for computer-predicted HAL values to estimate the actual risk of an injury is the subject of ongoing research. This method is advantageous over observational techniques since it does not depend on subjective judgement of an observer. Moreover, the hand speed equation, used by the computer algorithm, was more consistent with the HAL values obtained from observation than using the frequency of exertion (Akkas et al. 2015).

5. Conclusions

We conclude that automated video analytics can provide a good estimate of DC and HAL for actual industrial tasks. The video-based automated analysis was not just a good estimate of the human observed HAL, but also provided an objective and reliable estimate, since it did not depend on human judgement.

Disclosure statement

No potential conflict of interest was reported by the authors.

Funding

This work was supported, in part, by a grant from the National Institute for Occupational Safety and Health [grant number NIOSH/CDC, grant number R01OH011024 (Radwin)]. Additional support came from the National Institute for Occupational Safety and Health (NIOSH/CDC), R01OH007914 (Rempel).

ORCID

Robert G. Radwin http://orcid.org/0000-0002-7973-0641

References

ACGIH Worldwide. 2001. *Hand Activity Level TLV®*. Cincinnati, OH: ACGIH Worldwide.

Akkas, O., D. P. Azari, C.-H. Chen, Y. H. Hu, S. S. Ulin, T. J. Armstrong, D. Rempel, and R. G. Radwin. 2015. "A Hand Speed and Duty Cycle Equation for Estimating the ACGIH Hand Activity Level Rating." *Ergonomics* 58 (2): 184–194.

Akkas, O., C. H. Lee, Y. H. Hu, T. Y. Yen, and R. G. Radwin. 2016. "Measuring Elemental Time and Duty Cycle Using Automated Video Processing." *Ergonomics* 59: 1514–1525.

Bao, S., P. Spielholz, N. Howard, and B. Silverstein. 2006. "Quantifying Repetitive Hand Activityfor Epidemiological Research on Musculoskeletal Disorders–Part I: Individual Exposure Assessment." *Ergonomics* 49 (4): 361–380.

Bay, H., T. Tuytelaars, and L. Van Gool. 2006. "Surf: Speeded up Robust Features." In *European Conference on Computer Vision*, 404–417. Berlin: Springer, May.

Burt, Susan, Ken Crombie, Yan Jin, Steve Wurzelbacher, Jessica Ramsey, and James Deddens. 2011. "Workplace and Individual Risk Factors for Carpal Tunnel Syndrome." *Occupational and Environmental Medicine* 68 (12): 928–933.

Burt, S., J. A. Deddens, K. Crombie, Y. Jin, S. Wurzelbacher, and J. Ramsey. 2013. "A Prospective Study of Carpal Tunnel Syndrome: Workplace and Individual Risk Factors." *Occupational and Environmental Medicine* 70 (8): 568–574.

Chang, C. C., R. W. McGorry, J. H. Lin, X. Xu, and S. M. Hsiang. 2010. "Prediction Accuracy in Estimating Joint Angle Trajectories Using a Video Posture Coding Method for Sagittal Lifting Tasks." *Ergonomics* 53 (8): 1039–1047.

Chen, C. H., Y. H. Hu, and R. G. Radwin. 2014. "A Motion Tracking System for Hand Activity Assessment." In Signal and Information Processing (ChinaSIP), 2014 IEEE China Summit & International Conference on July, Xi'an, China: IEEE, 320–324).

Chen, C. H., Y. H. Hu, T. Y. Yen, and R. G. Radwin. 2013. "Automated video exposure assessment of repetitive hand activity level for a load transfer task." *Human factors* 55 (2): 298–308.

Coelho, D. A., C. Harris-Adamson, T. M. Lima, I. Janowitz, and D. M. Rempel. 2013. "Correlation Between Different Hand Force Assessment Methods from an Epidemiological Study." *Human Factors and Ergonomics in Manufacturing & Service Industries* 23 (2): 128–139.

Dale, A. M., K. Miller, B. T. Gardner, C. T. Hwang, B. Evanoff, and L. Welch. 2016. "Observed Use of Voluntary Controls to Reduce Physical Exposures among Sheet Metal Workers of the Mechanical Trade." *Applied Ergonomics* 52: 69–76.

Dartt, A., J. Rosecrance, F. Gerr, P. Chen, D. Anton, and L. Merlino. 2009. "Reliability of Assessing Upper Limb Postures

among Workers Performing Manufacturing Tasks." *Applied Ergonomics* 40 (3): 371–378.

David, G. C. 2005. "Ergonomic Methods for Assessing Exposure to Risk Factors for Work-related Musculoskeletal Disorders." *Occupational Medicine* 55 (3): 190–199.

Dempsey, P. G., R. W. McGorry, and W. S. Maynard. 2005. "A survey of tools and methods used by certified professional ergonomists." *Applied ergonomics* 36 (4): 489–503.

Ebersole, M. L., and T. J. Armstrong. 2002. "Inter-Rater Reliability for Hand Activity Level (HAL) and Force Metrics." In *Proceedings of the Human Factors and Ergonomics Society Annual Meeting*, Vol. 46, No. 13, 1037–1040. SAGE Publications, September.

Estember, R. D., R. T. Panugot, and A. D. Vale. 2015. "The Musculoskeletal Disorder Effects on the Use of Single and Dual Monitor Workstations." In *Industrial Engineering and Operations Management (IEOM), 2015 International Conference on*, 1–7. IEEE, March.

Fan, Z. J., B. A. Silverstein, S. Bao, D. K. Bonauto, N. L. Howard, and C. K. Smith. 2014. "The Association between Combination of Hand Force and Forearm Posture and Incidence of Lateral Epicondylitis in a Working Population." *Human Factors* 56 (1): 151–165.

Fischler, M. A., and R. C. Bolles. 1981. "Random Sample Consensus: A Paradigm for Model Fitting with Applications to Image Analysis and Automated Cartography." *Communications of the ACM* 24 (6): 381–395.

Harris, C., E. A. Eisen, R. Goldberg, N. Krause, and D. Rempel. 2011. "1st Place, PREMUS Best Paper Competition: Workplace and Individual Factors in Wrist Tendinosis among Blue-collar Workers – The San Francisco Study." *Scandinavian Journal of Work Environment Health* 37 (2): 85–98.

Harris-Adamson, C., D. You, E. A. Eisen, R. Goldberg, and D. Rempel. 2013. "The Impact of Posture on Wrist Tendinosis among Blue-collar Workers the San Francisco Study." *Human Factors: The Journal of the Human Factors and Ergonomics Society*, 0018720813502807.

Harris-Adamson, C., E. A. Eisen, J. Kapellusch, A. Garg, K. T. Hegmann, M. S. Thiese, A. M. Dale, B. Evanoff, S. Burt, S. Bao, B. Silverstein, L. Merlino, F. Gerr, and D. Rempel. 2015. "Biomechanical Risk Factors for Carpal Tunnel Syndrome: A Pooled Study of 2474 Workers." *Occupational and Environmental Medicine* 72 (1): 33–41.

Latko, W. A., T. J. Armstrong, J. A. Foulke, G. D. Herrin, R. A. Rabourn, and S. S. Ulin. 1997. "Development and Evaluation of an Observational Method for Assessing Repetition in Hand Tasks." *American Industrial Hygiene Association Journal* 58 (4): 278–285.

Lu, M. L., S. Sudhakaran, and M. Aep. 2005. "Evaluation of the Effectiveness of a Redesigned Pipette for Reducing the Risk Factors for Musculoskeletal Disorders." *Applied Ergonomics*.

Lu, M. L., T. James, B. Lowe, M. Barrero, and Y. K. Kong. 2008. "An Investigation of Hand Forces and Postures for Using Selected Mechanical Pipettes." *International Journal of Industrial Ergonomics* 38 (1): 18–29.

Marras, William S., Robert G. Cutlip, Susan E. Burt, and Thomas R. Waters. 2009. "National Occupational Research Agenda (NORA) Future Directions in Occupational Musculoskeletal Disorder Health Research." Applied Ergonomics 40 (1): 15–22.

McGaha, Jamie, Kim Miller, Alexis Descatha, Laurie Welch, Bryan Buchholz, Bradley Evanoff, and Ann Marie Dale. 2014. "Exploring Physical Exposures and Identifying High-Risk Work Tasks within the Floor Layer Trade." *Applied Ergonomics* 45 (4): 857–864.

Paquet, V. L., S. E. Mathiassen, and P. G. Dempsey. 2006. "Video-based Ergonomic Job Analysis: A Practitioner's Guide." *Professional Safety* 51 (11): 27.

Paulsen, R., N. Schwatka, J. Gober, D. Gilkey, D. Anton, F. Gerr, and J. Rosecrance. 2014. "Inter-rater Reliability of Cyclic and Non-cyclic Task Assessment Using the Hand Activity Level in Appliance Manufacturing." *International Journal of Industrial Ergonomics* 44 (1): 32–38.

Punnett, L., and D. H. Wegman. 2004. "Work-related Musculoskeletal Disorders: The Epidemiologic Evidence and the Debate." *Journal of Electromyography and Kinesiology* 14 (1): 13–23.

Radwin, R. G., D. P. Azari, M. J. Lindstrom, S. S. Ulin, T. J. Armstrong, and D. Rempel. 2015. "A Frequency–Duty Cycle Equation for the ACGIH Hand Activity Level." *Ergonomics* 58 (2): 173–183.

Rao, C., A. Yilmaz, and M. Shah. 2002. "View-invariant Representation and Recognition of Actions." *International Journal of Computer Vision* 50 (2): 203–226.

Silverstein, Barbara A., Z. Joyce Fan, Dave K. Bonauto, Stephen Bao, Caroline K. Smith, Ninica Howard, and Eira Viikari-Juntura 2010. "The Natural Course of Carpal Tunnel Syndrome in a Working Population." *Scandinavian Journal of Work, Environment & Health* 384–393.

Spielholz, Peregrin, Barbara Silverstein, Michael Morgan, Harvey Checkoway, and Joel Kaufman. 2001. "Comparison of Self-Report, Video Observation and Direct Measurement Methods for Upper Extremity Musculoskeletal Disorder Physical Risk Factors." *Ergonomics* 44 (6): 588–613.

Spielholz, P., S. Bao, N. Howard, B. Silverstein, J. Fan, C. Smith, and C. Salazar. 2008. "Reliability and Validity Assessment of the Hand Activity Level Threshold Limit Value and Strain Index Using Expert Ratings of Mono-task Jobs." *Journal of Occupational and Environmental Hygiene* 5 (4): 250–257.

Story, M. F., J. M. Winters, M. R. Lemke, A. Barr, E. Omiatek, I. Janowitz, A. Brafman, and D. Rempel. 2010. "Development of a Method for Evaluating Accessibility of Medical Equipment for Patients with Disabilities." *Applied Ergonomics* 42 (1): 178–183.

Torr, P. H., and A. Zisserman. 2000. "MLESAC: A New Robust Estimator with Application to Estimating Image Geometry." *Computer Vision and Image Understanding* 78 (1): 138–156.

Yen, T. Y., and R. G. Radwin. 1995. "A Video-Based System for Acquiring Biomechanical Data Synchronized with Arbitrary Events and Activities." *IEEE Transactions on Biomedical Engineering* 42 (9): 944–948.

Yen, T. Y., and R. G. Radwin. 2006. "12 Usability Testing by Multimedia Video Task Analysis." *Medical Instrumentation: Accessibility and Usability Considerations*, 159.